PERIODICA POLYTECHNICA SER. MECH. ENG. VOL. 48, NO. 1, PP. 27–39 (2004)

STABILITY TRANSITION BETWEEN 1 AND 2 DEGREE-OF-FREEDOM MODELS OF MILLING

Tamás INSPERGER*[1] and Gábor STÉPÁN**

*Department of Applied Mechanics
Budapest University of Technology and Economics
H–1521 Budapest, Hungary
Phone: +36 1 463 1227, Fax: +36 1 463 3471
e-mail: inspi@mm.bme.hu
http://www.mm.bme.hu/~inspi

**Department of Applied Mechanics
Budapest University of Technology and Economics
H–1521 Budapest, Hungary
Phone: +36 1 463 1369, Fax: +36 1 463 3471
e-mail: stepan@mm.bme.hu
http://www.mm.bme.hu/~stepan

Received: Dec. 10, 2003

Abstract

Chatter prediction for 2 degree of freedom (DOF) milling model is presented. The workpiece is assumed to be flexible and the tool to be stiff. Non-linear cutting force model is used, and the linearized equation of motion is derived. Stability charts are constructed for different stiffness values in the directions x and y. The charts for the 1 DOF models associated with the x and the y directions are also given. It is shown that the 2-DOF case can not be given via the pure overlaying of the charts of the two single DOF cases.

Keywords: milling, dynamics, chatter, stability.

1. Introduction

The rapid development of machining technology during the past decade, and the commercialization of reliable high-speed machining systems have driven the need for thorough dynamical investigation of high-speed cutting processes. One important phenomenon that limits the productivity of machining is the arising self-excited vibration, called regenerative machine tool chatter. The work of TLUSTY et al. (1962), TOBIAS (1965) and KUDINOV (1955) led to the development of the 'stability lobe diagram' that plots the boundary between stable and unstable cuts as a function of spindle speed and depth of cut.

Analytical prediction of chatter in milling processes is extremely difficult. The accurate modelling of the regenerative effect leads to a delay-differential equation (DDE) with a corresponding infinite dimensional state space (STÉPÁN, 1989).

[1] all correspondence to this author

Due to the periodic excitation of rotating teeth of the miller, the governing equation of milling is a DDE with time-periodic coefficients. Closed form stability conditions can not be given for the general milling case. Usually, numerical simulations (SMITH and TLUSTY, 1991, ZHAO and BALACHANDRAN, 2001, PEIGNÉ et al., 2003) and different analytical techniques (ALTINTAS et al., 1999, TIAN and HUTTON, 2001, DAVIES et al., 2002, INSPERGER et al., 2003a, MANN et al., 2003a, 2003b, BAYLY et al., 2003, CORPUS and ENDRES, 2003, SZALAI and STÉPÁN, 2003, WANG et al., 2003, FAASSEN et al. 2003) are used to derive stability charts.

Vibrations arise due to the flexible parts in the system, like tool, tool holder, workpiece, etc. For some simple cases, when a well defined first mode is dominant, like milling a thin walled workpiece with a stiff miller, the 1 degree of freedom (DOF) assumption is satisfactory. In this case the stability chart consists of an infinite series of stability lobes that are associated to either secondary Hopf or period doubling (flip) bifurcation. The analysis of the vibration frequencies (INSPERGER et al., 2003b) and the chatter signal (GRADIŠEK et al., 2002) resulted in a deep understanding of the 1 DOF case.

Usually, there is no well defined dominant mode of the tool-workpiece system, and the process can only be modelled as a multi-DOF system. An example is when the tool is the most flexible part, and it is modelled as a cantilever beam (KIVANC and BUDAK, 2003). In this case a 2 DOF model is considered with the same (or almost same) parameters in the x and y directions and diagonal modal matrices arise in the equation of motion. However, if the tool is not symmetric, and the modal parameters are different in the two principal directions, then the corresponding modal matrices in the equation of motion are not diagonal, but time-periodic due to the rotation of the tool. If the tool is stiff and the workpiece is flexible with two dominant modes, then the 2 DOF model can also be used. In this case, the modal parameters may also differ for the two modes. For these cases the stability charts are more complex than those of the 1 DOF case, since both the x and y directions can be associated to an infinite series of stability lobes, and the resultant stability chart is a complex combination of these two sets of lobes.

If further higher modes also take important role in the system dynamics, then the structure of the stability charts are even more complicated. For these cases the estimation of the modal parameters needs a sophisticated modal analysis of the complex structure of the tool, the tool-holder and the workpiece (SCHMITZ et al., 2001, ESTERLING et al., 2003, YOUNG and HELVEY, 2003).

In the present study a 2 DOF model is considered with a stiff tool and a flexible workpiece. The non-linear cutting force model is used, and the linearized equation of motion is derived. Stability charts are constructed for different stiffness values in the directions x and y. The charts for the 1 DOF models assigned to the x and the y directions are also given. It is shown that the 2 DOF case can not be given by the pure overlaying of the lobes of the two 1 DOF cases.

2. Mechanical Model

The 2 DOF mechanical model of milling is shown in *Fig, 1*. The workpiece is assumed to be flexible relative to the milling table with dominant modes parallel (x) and perpendicular (y) to the feed. The modal mass of the workpiece is m, the stiffness and damping are k_x, c_x, k_y and c_y for both x and y directions. The linear feed motion of the milling table is described by vt. The equation of motion reads

$$m\ddot{x}(t) + c_x\dot{x}(t) + k_x x(t) = F_x(t)\,, \tag{1}$$
$$m\ddot{y}(t) + c_y\dot{y}(t) + k_y y(t) = F_y(t)\,. \tag{2}$$

Here x and y denote the position of the workpiece relative to the milling table. The cutting forces $F_x(t)$ and $F_y(t)$ are time-dependent due to the rotation of the tool. Note that the case investigated here is a special one. Usually, the dominant modes are neither parallel nor perpendicular to the feed, and cross modal terms are arising in the equation.

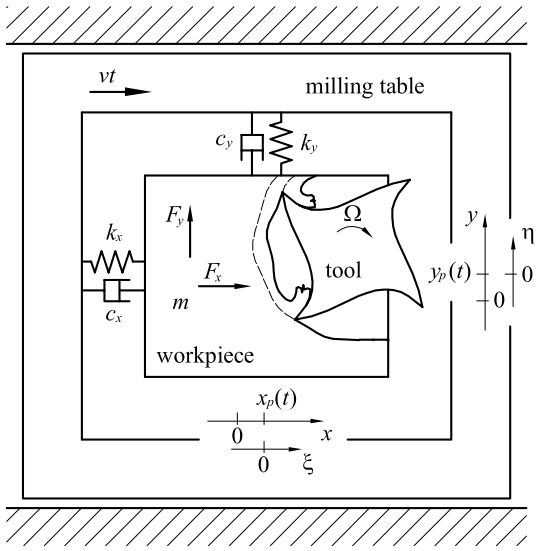

Fig. 1. Mechanical model

The helix angle is also included in the model. The cutter is modelled as a stack of infinitesimal (differential) disk elements. A differential element along the depth of cut is shown in *Fig. 2*. The tangential and the normal forces acting on this differential element are

$$\mathrm{d}F_{j\,t}(t,z) = g(\varphi_j(t,z))K_t(f(t,z))^{x_F}\,\mathrm{d}z\,, \tag{3}$$
$$\mathrm{d}F_{j\,n}(t,z) = g(\varphi_j(t,z))K_n(f(t,z))^{x_F}\,\mathrm{d}z\,, \tag{4}$$

where K_t and K_n are the tangential and the normal cutting coefficients, respectively, $f(t,z)$ is the chip thickness and the exponent x_F is a constant ($x_F = 0.8$ is a typical value for this parameter). The angular position of the cutting edge j corresponding to the investigated differential element of the tool is

$$\varphi_j(t,z) = \frac{2\pi\Omega}{60}t - \frac{z\tan\gamma}{R} + j\frac{2\pi}{N}, \tag{5}$$

where Ω is the spindle speed in [rpm], z denotes the axial direction, γ is the helix angle (see *Fig. 2*), R is the radius of the tool and N is the number of teeth. The function $g_j(t)$ is a screen function, it is equal to 1, if the jth tooth is active, and it is 0, if not:

$$g(\varphi_j(t,z)) = \begin{cases} 1 & \text{if} \quad \varphi_{\text{enter}} < \varphi_j(t,z) < \varphi_{\text{exit}} \\ 0 & \text{otherwise} \end{cases}, \tag{6}$$

where φ_{enter} and φ_{exit} are the angles where the teeth enter and exit the cut, respectively.

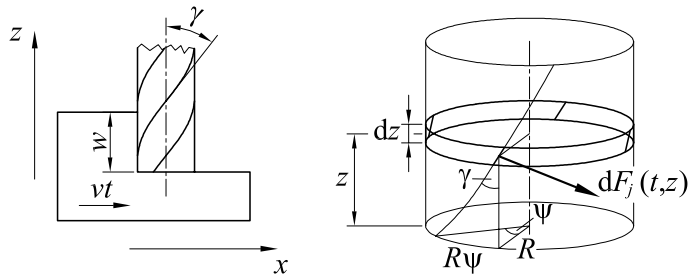

Fig. 2. Differential element of the tool modelling the helix angle

The x and y components of the differential cutting force are given as (see *Fig. 3*)

$$\mathrm{d}F_{jx}(t,z) = \mathrm{d}F_{jt}(t,z)\cos\varphi_j(t,z) + \mathrm{d}F_{jn}(t,z)\sin\varphi_j(t,z), \tag{7}$$

$$\mathrm{d}F_{jy}(t,z) = -\mathrm{d}F_{jt}(t,z)\sin\varphi_j(t,z) + \mathrm{d}F_{jn}(t,z)\cos\varphi_j(t,z). \tag{8}$$

If $v\tau \ll R$, where $v\tau$ is the feed per tooth, then the chip thickness can be expressed according to *Fig. 4* as

$$\begin{aligned} f(\varphi_j(t,z)) &= A\sin\varphi_j(t,z) + B\cos\varphi_j(t,z) \\ &= (v\tau + x(t-\tau) - x(t))\sin\varphi_j(t,z) + (y(t-\tau) - y(t))\cos\varphi_j(t,z), \end{aligned} \tag{9}$$

where $\tau = 60/(N\Omega)$ is the tooth passing period.

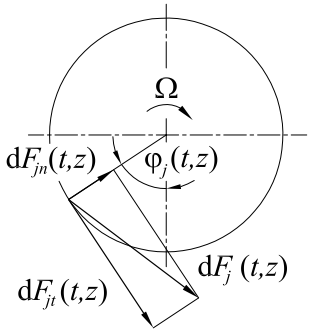

Fig. 3. Cutting force model

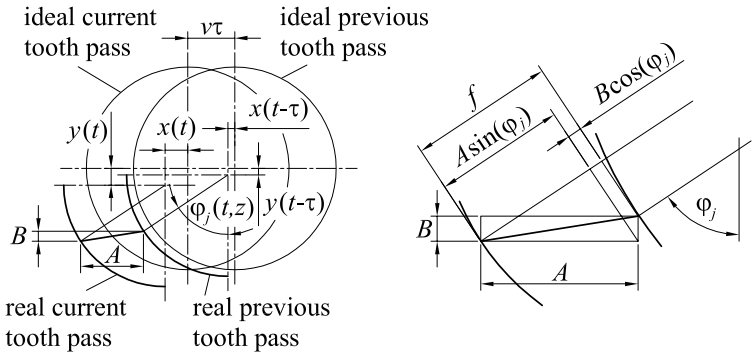

Fig. 4. Chip thickness model

The cutting force acting on tooth j is obtained by integration of *Eqs.* (7) and (8) along the axial direction:

$$\begin{aligned} F_{j\,x}(t) &= \int_0^w \mathrm{d}F_{j,x}(t,z) \\ &= \int_0^w g(\varphi_j(t,z))(f(t,z))^{x_F}\left(K_t\cos\varphi_j(t,z) + K_n\sin\varphi_j(t,z)\right)\mathrm{d}z\,, \quad (10) \\ F_{j\,y}(t) &= \int_0^w \mathrm{d}F_{j,y}(t,z) \\ &= \int_0^w g(\varphi_j(t,z))(f(t,z))^{x_F}\left(-K_t\sin\varphi_j(t,z) + K_n\cos\varphi_j(t,z)\right)\mathrm{d}z\,, \\ & \quad (11) \end{aligned}$$

where w is the axial depth of cut. The resultant forces are the sum of the forces

acting on the teeth:

$$F_x(t) = \sum_{j=1}^{N} F_{j\,x}(t)\,, \quad \text{and} \quad F_y(t) = \sum_{j=1}^{N} F_{j\,y}(t). \tag{12}$$

The equations of motion can be written in the forms:

$$\begin{aligned} &m\ddot{x}(t) + c_x\dot{x}(t) + k_x x(t) \\ &\quad = \sum_{j=1}^{N} \int_0^w g(\varphi_j(t,z))\big(K_t \cos\varphi_j(t,z) + K_n \sin\varphi_j(t,z)\big) \\ &\qquad \times\Big(\big(v\tau + x(t-\tau) - x(t)\big)\sin\varphi_j(t,z) \\ &\qquad +\big(y(t-\tau) - y(t)\big)\cos\varphi_j(t,z)\Big)^{x_F}\,\mathrm{d}z\,, \end{aligned} \tag{13}$$

$$\begin{aligned} &m\ddot{y}(t) + c_y\dot{y}(t) + k_y y(t) \\ &\quad = \sum_{j=1}^{N} \int_0^w g(\varphi_j(t,z))\big(-K_t \sin\varphi_j(t,z) + K_n \cos\varphi_j(t,z)\big) \\ &\qquad \times\Big(\big(v\tau + x(t-\tau) - x(t)\big)\sin\varphi_j(t,z) \\ &\qquad +\big(y(t-\tau) - y(t)\big)\cos\varphi_j(t,z)\Big)^{x_F}\,\mathrm{d}z\,. \end{aligned} \tag{14}$$

Now, the motion of the workpiece is assumed to be in the form:

$$x(t) = x_p(t) + \xi(t)\,, \tag{15}$$

$$y(t) = y_p(t) + \eta(t)\,, \tag{16}$$

where $x_p(t+\tau) = x_p$ and $y_p(t+\tau) = y_p(t)$ are periodic functions, $\xi(t)$ and $\eta(t)$ are perturbations associated with machine tool chatter in the x and the y directions, respectively. Substitution of *Eqs.* (15) and (16) into *Eqs.* (13) and (14) results in

$$\begin{aligned} &m\ddot{x}_p(t) + c_x\dot{x}_p(t) + k_x x_p(t) + m\ddot{\xi}(t) + c_x\dot{\xi}(t) + k_x\xi(t) \\ &\quad = \sum_{j=1}^{N} \int_0^w g(\varphi_j(t,z))\big(K_t \cos\varphi_j(t,z) + K_n \sin\varphi_j(t,z)\big) \\ &\qquad \times\Big(\big(v\tau + \xi(t-\tau) - \xi(t)\big)\sin\varphi_j(t,z) \\ &\qquad +\big(\eta(t-\tau) - \eta(t)\big)\cos\varphi_j(t,z)\Big)^{x_F}\,\mathrm{d}z\,, \end{aligned} \tag{17}$$

$$
\begin{aligned}
&m\ddot{y}_p(t) + c_y\dot{y}_p(t) + k_y y_p(t) + m\ddot{\eta}(t) + c_y\dot{\eta}(t) + k_y\eta(t) \\
&\quad = \sum_{j=1}^{N}\int_0^w g(\varphi_j(t,z))\big(-K_t\sin\varphi_j(t,z) + K_n\cos\varphi_j(t,z)\big) \\
&\qquad \times\Big(\big(v\tau + \xi(t-\tau) - \xi(t)\big)\sin\varphi_j(t,z) \\
&\qquad +\big(\eta(t-\tau) - \eta(t)\big)\cos\varphi_j(t,z)\Big)^{x_F}\,\mathrm{d}z\,. \qquad (18)
\end{aligned}
$$

For the ideal case, when no chatter arises, the motion is described by $x(t) = x_p(t)$ and $y(t) = y_p(t)$, and the equations of motion are

$$
\begin{aligned}
&m\ddot{x}_p(t) + c_x\dot{x}_p(t) + k_x x_p(t) \\
&\quad = \sum_{j=1}^{N}\int_0^w g(\varphi_j(t,z))\big(K_t\cos\varphi_j(t,z) \\
&\qquad +K_n\sin\varphi_j(t,z)\big)\Big(\big(v\tau\big)\sin\varphi_j(t,z)\Big)^{x_F}\,\mathrm{d}z\,, \qquad (19)
\end{aligned}
$$

$$
\begin{aligned}
&m\ddot{y}_p(t) + c_y\dot{y}_p(t) + k_y y_p(t) \\
&\quad = \sum_{j=1}^{N}\int_0^w g(\varphi_j(t,z))\big(-K_t\sin\varphi_j(t,z) \\
&\qquad +K_n\cos\varphi_j(t,z)\big)\Big(\big(v\tau\big)\sin\varphi_j(t,z)\Big)^{x_F}\,\mathrm{d}z\,. \qquad (20)
\end{aligned}
$$

For linear stability analysis, the variational system of *Eqs.* (13) and (14) is determined for the periodic motion $\big(x_p(t),\ y_p(t)\big)$. Expand the non-linear term in *Eqs.* (17) and (18) into Taylor series with respect to $\big(\xi(t),\eta(t)\big)$, and neglect the higher order terms to get

$$
\begin{aligned}
&m\ddot{x}_p(t) + c_x\dot{x}_p(t) + k_x x_p(t) + m\ddot{\xi}(t) + c_x\dot{\xi}(t) + k_x\xi(t) \\
&\quad = \sum_{j=1}^{N}\int_0^w g(\varphi_j(t,z))\big(K_t\cos\varphi_j(t,z) + K_n\sin\varphi_j(t,z)\big) \\
&\qquad \times\Big(\big(v\tau\sin\varphi_j(t,z)\big)^{x_F} + \Big(x_F\big(v\tau\sin\varphi_j(t,z)\big)^{x_F-1}\sin\varphi_j(t,z)\Big) \\
&\qquad \times\big(\xi(t-\tau) - \xi(t)\big) + \Big(x_F\big(v\tau\sin\varphi_j(t,z)\big)^{x_F-1}\cos\varphi_j(t,z)\Big) \\
&\qquad \times\big(\eta(t-\tau) - \eta(t)\big)\Big)\,\mathrm{d}z\,, \qquad (21)
\end{aligned}
$$

$$
\begin{aligned}
&m\ddot{y}_p(t) + c_y\dot{y}_p(t) + k_y y_p(t) + m\ddot{\eta}(t) + c_y\dot{\eta}(t) + k_y\eta(t)\\
&\quad = \sum_{j=1}^{N}\int_0^w g(\varphi_j(t,z))\big(-K_t\sin\varphi_j(t,z) + K_n\cos\varphi_j(t,z)\big)\\
&\qquad \times\Big(\big(v\tau\sin\varphi_j(t,z)\big)^{x_F} + \Big(x_F\big(v\tau\sin\varphi_j(t,z)\big)^{x_F-1}\sin\varphi_j(t,z)\Big)\\
&\qquad \times\big(\xi(t-\tau)-\xi(t)\big) + \Big(x_F\big(v\tau\sin\varphi_j(t,z)\big)^{x_F-1}\cos\varphi_j(t,z)\Big)\\
&\qquad \times\big(\eta(t-\tau)-\eta(t)\big)\Big)\,\mathrm{d}z\,. \qquad (22)
\end{aligned}
$$

Using *Eqs.* (19), (20) and (21), (22), a linear periodic DDE is obtained for $\big(\xi(t),\,\eta(t)\big)$ as

$$
\begin{aligned}
&m\ddot{\xi}(t) + c_x\dot{\xi}(t) + k_x\xi(t)\\
&\quad = h_{xx}(t)\big(\xi(t-\tau)-\xi(t)\big) + h_{xy}(t)\big(\eta(t-\tau)-\eta(t)\big)\,, \qquad (23)\\
&m\ddot{\eta}(t) + c_y\dot{\eta}(t) + k_y\eta(t)\\
&\quad = h_{yx}(t)\big(\xi(t-\tau)-\xi(t)\big) + h_{yy}(t)\big(\eta(t-\tau)-\eta(t)\big)\,, \qquad (24)
\end{aligned}
$$

where

$$
\begin{aligned}
h_{xx}(t) &= \sum_{j=1}^{N}\int_0^w g(\varphi_j(t,z))\big(K_t\cos\varphi_j(t,z) + K_n\sin\varphi_j(t,z)\big)\\
&\quad\times\Big(x_F\big(v\tau\sin\varphi_j(t,z)\big)^{x_F-1}\sin\varphi_j(t,z)\Big)\,\mathrm{d}z\,, \qquad (25)\\
h_{xy}(t) &= \sum_{j=1}^{N}\int_0^w g(\varphi_j(t,z))\big(K_t\cos\varphi_j(t,z) + K_n\sin\varphi_j(t,z)\big)\\
&\quad\times\Big(x_F\big(v\tau\sin\varphi_j(t,z)\big)^{x_F-1}\cos\varphi_j(t,z)\Big)\,\mathrm{d}z\,, \qquad (26)\\
h_{yx}(t) &= \sum_{j=1}^{N}\int_0^w g(\varphi_j(t,z))\big(-K_t\sin\varphi_j(t,z) + K_n\cos\varphi_j(t,z)\big)\\
&\quad\times\Big(x_F\big(v\tau\sin\varphi_j(t,z)\big)^{x_F-1}\sin\varphi_j(t,z)\Big)\,\mathrm{d}z\,, \qquad (27)\\
h_{yy}(t) &= \sum_{j=1}^{N}\int_0^w g(\varphi_j(t,z))\big(-K_t\sin\varphi_j(t,z) + K_n\cos\varphi_j(t,z)\big)\\
&\quad\times\Big(x_F\big(v\tau\sin\varphi_j(t,z)\big)^{x_F-1}\cos\varphi_j(t,z)\Big)\,\mathrm{d}z\,. \qquad (28)
\end{aligned}
$$

Finally, *Eqs.* (23) and (24) are put in the following vector form:

$$\begin{pmatrix} m & 0 \\ 0 & m \end{pmatrix} \begin{pmatrix} \ddot{\xi}(t) \\ \ddot{\eta}(t) \end{pmatrix} + \begin{pmatrix} c_x & 0 \\ 0 & c_y \end{pmatrix} \begin{pmatrix} \dot{\xi}(t) \\ \dot{\eta}(t) \end{pmatrix} + \begin{pmatrix} k_x + h_{xx}(t) & h_{xy}(t) \\ h_{yx}(t) & k_y + h_{yy}(t) \end{pmatrix} \begin{pmatrix} \xi(t) \\ \eta(t) \end{pmatrix} = \begin{pmatrix} h_{xx}(t) & h_{xy}(t) \\ h_{yx}(t) & h_{yy}(t) \end{pmatrix} \begin{pmatrix} \xi(t-\tau) \\ \eta(t-\tau) \end{pmatrix} . \tag{29}$$

3. Stability Charts

The stability analysis was carried out by the semi-discretization method (INSPERGER and STÉPÁN, 2002). Stability charts are determined for the parameters summarized in *Table 1*.

Table 1. Parameters used for stability chart construction

tool diameter	$D = 2R$=12.25 [mm]
number of teeth	N=2
helix angle	γ=25°
cutting force exponent	x_F=0.75
feed per tooth	$v\tau$=0.1 [mm]
tangential cutting coefficient	K_t=6e7 [N/m$^{1+x_F}$]
normal cutting coefficient	K_n=2e7 [N/m$^{1+x_F}$]
modal mass	m=0.1 [mm]
damping in direction x	c_x=6 [Ns/m]
damping in direction y	c_y=6 [Ns/m]

The system is investigated with different stiffness values in both x and y directions. *Table 2* shows the stiffness values and the corresponding natural frequencies of the investigated cases. Case (b) corresponds to a symmetric tool, while for case (a) and (c) $f_y = 2f_x$ and $f_x = 2f_y$, respectively.

Table 2. Stiffness parameters and the associated natural frequencies used for stability chart construction

case	k_x	k_y	f_x	f_y
(a)	3×10^6 N/m	12×10^6 N/m	329.48 Hz	658.96 Hz
(b)	3×10^6 N/m	3×10^6 N/m	329.48 Hz	329.48 Hz
(c)	12×10^6 N/m	3×10^6 N/m	658.96 Hz	329.48 Hz

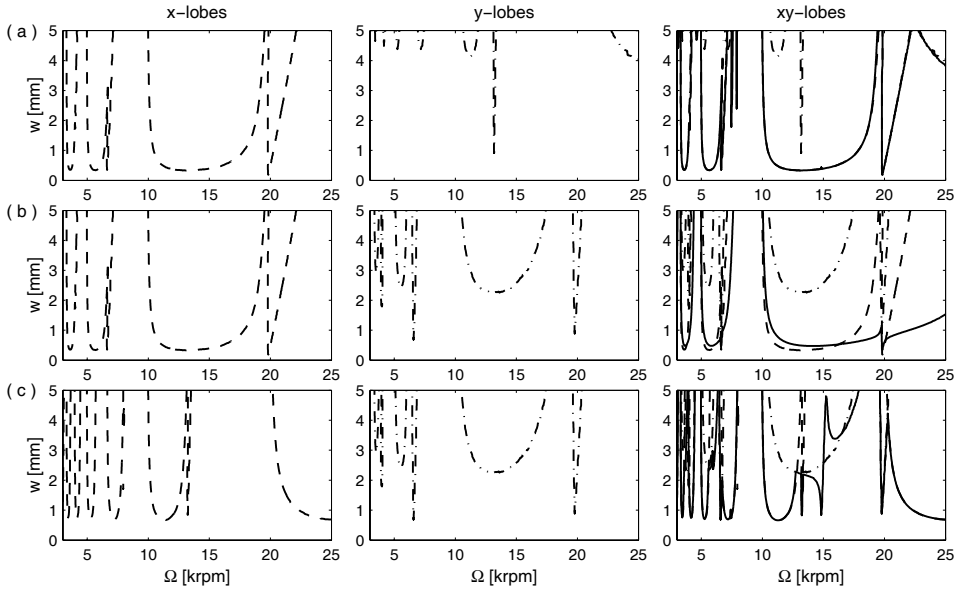

Fig. 5. Stability charts for 10% radial immersion up-milling

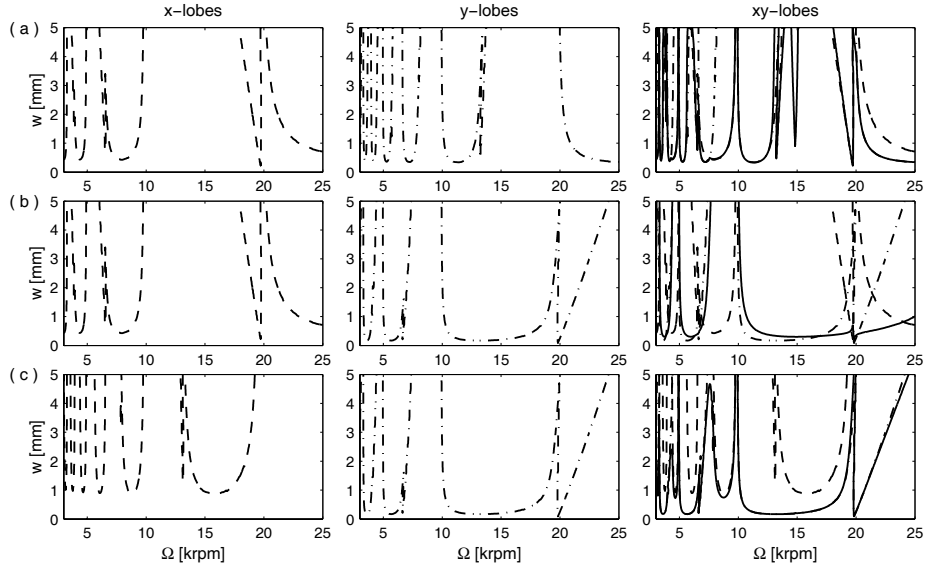

Fig. 6. Stability charts for 10% radial immersion down-milling

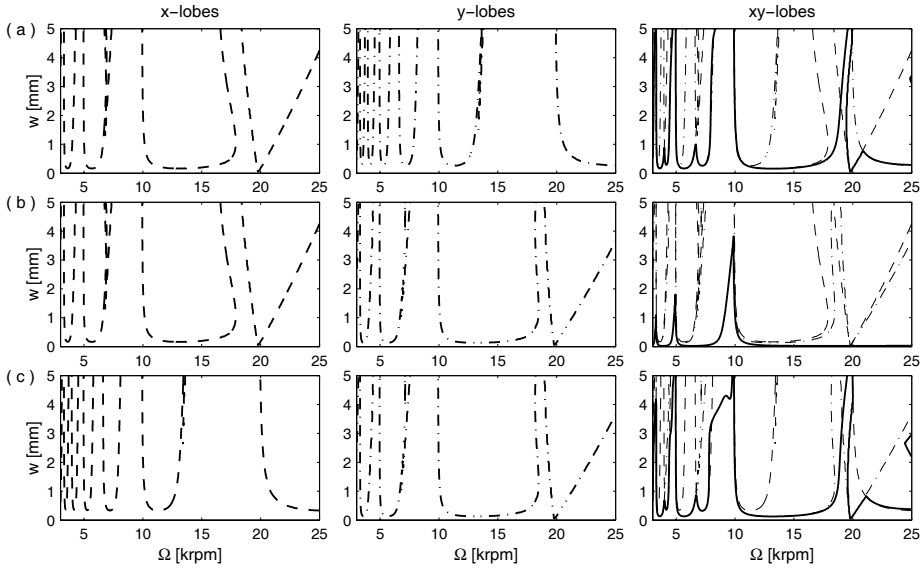

Fig. 7. Stability charts for full immersion milling

The resulting stability charts for 10% radial immersion up- and down-milling and for full immersion milling are shown in *Figs.* 5, 6 and 7. Cases (a), (b) and (c) refer to the parameters given in *Table* 2. In the charts titled as x-lobes, the stability boundaries of a 1 DOF case with flexible x direction can be seen (dashed lines). The charts titled as y-lobes show the stability boundaries of a 1 DOF case with flexible y direction (dash-dotted lines). These 1 DOF cases are also considered in MANN et al. (2003c). The charts titled as xy-lobes present the stability boundaries of the 2 DOF case with flexible x and y directions (continuous lines). For comparison, the 1 DOF cases are also presented in the xy-lobe plots by dashed and dash-dotted lines.

4. Conclusions

As it can be seen in *Figs.* 5, 6 and 7, the stability behaviour depends strongly on the flexibility of both x and y directions. Since the x and y modes are coupled through the cutting force, the 2 DOF stability boundaries can not be given by a pure overlaying of the x- and y-lobes of the 1 DOF cases, as it can also be seen in the plots of xy-lobes in *Figs.* 5, 6 and 7. However, for the cases (a) and (c), when the natural frequencies in the x and y directions are different, some parts of the xy-lobes seem to be the same as either the x- or the y-lobes. For case (b) the difference between the 1 DOF cases and the 2 DOF case is more essential. The

explanation is that cases (a) and (c) are more decoupled than case (b).

As the difference between the stiffness values in the x and y direction is increased, and the system gets more and more decoupled, the stability charts converge to those of the 1 DOF cases of either the x or the y flexibility.

Acknowledgements

This research was supported in part by the Magyary Zoltán Postdoctoral Fellowship of Foundation for Hungarian Higher Education and Research and by the Hungarian National Science Foundation under grant no. OTKA T043368 and OTKA F047318.

References

[1] ALTINTAS, Y. – ENGIN, S. – BUDAK, E., Analytical Stability Prediction and Design of Variable Pitch Cutters, *Journal of Manufacturing Science and Engineering* **121** (1999), pp. 173–178.

[2] BAYLY, P. V. – HALLEY, J. E. – MANN, B. P. – DAVIES, M. A., Stability of Interrupted Cutting by Temporal Finite Element Analysis, *Journal of Manufacturing Science and Engineering* **125**(2) (2003), pp. 220–225.

[3] CORPUS, W. T. – ENDRES, W. J., An Analytical Model to Predict Chatter in Multi-Dimensional Periodically Time-Varying Machining Processes, in *Proceedings of the 2003 ASME International Mechanical Engineering Congress and Exposition, Washington, DC*, (2003), paper no. IMECE2003-42488 (CD-ROM).

[4] DAVIES, M. A. – PRATT, J. R. – DUTTERER, B. – BURNS, T. J., Stability Prediction for Low Radial Immersion Milling, *Journal of Manufacturing Science and Engineering* **124**(2) (2002), pp. 217–225.

[5] ESTERLING, D. – CAULFIELD, F. D. – KIEFER, A. – BUCKNER, G. – JAJU, P., Non-Contact Device for Measuring Frequency Response Functions of CNC Machine Tools, in *Proceedings of the 2003 ASME International Mechanical Engineering Congress and Exposition, Washington, DC*, (2003), paper no. IMECE2003-42265 (CD-ROM).

[6] FAASSEN, R. P. H. – VAN DE WOUW, N. – OOSTERLING, J. A. J. – NIJMEIJER, H., Prediction of Regenerative Chatter by Modelling and Analysis of High-Speed Milling, *International Journal of Machine Tools and Manufacture*, **43**(14) (2003), pp. 1437–1446.

[7] GRADIŠEK, J. – FRIEDRICH, R. – GOVEKAR, E. – GRABEC, I., Analysis of Data from Periodically Forced Stochastic Processes, *Physics Letters A* **294**(3–4) (2002), pp. 234–238.

[8] INSPERGER, T. – STÉPÁN, G., Semi-Discretization Method for Delayed Systems, *International Journal for Numerical Methods in Engineering* **55**(5) (2002), pp. 503–518.

[9] INSPERGER, T. – MANN, B. P. – STÉPÁN, G. – BAYLEY, P. V., Stability of Up-Milling and Down-Milling, Part 1: Alternative Analytical Methods, *International Journal of Machine Tools and Manufacture* **43**(1) (2003), pp. 25–34.

[10] INSPERGER, T. – STÉPÁN, G. – BAYLY, P. V. – MANN, B. P., Multiple Chatter Frequencies in Milling Processes, *Journal of Sound and Vibration*, **262**(2) (2003), pp. 333–345.

[11] KIVANC, E. B. – BUDAK, E., Development of Analytical Endmill Deflection and Dynamic Models, in *Proceedings of the 2003 ASME International Mechanical Engineering Congress and Exposition, Washington, DC*, (2003), paper no. IMECE2003-42301 (CD-ROM).

[12] KUDINOV, V. A., *Theory of Vibration Generated from Metal Cutting* (in Russian), New Technology of Mechanical Engineering, Moscow: USSR Academy of Sciences Publishing House 1-7, 1955.

[13] MANN, B. P. – INSPERGER, T. – BAYLY, P. V. – STÉPÁN, G., Stability of Up-Milling and Down-Milling, Part 2: Experimental Verification, *International Journal of Machine Tools and Manufacture*, **43**(1) (2003), pp. 35–40.
[14] MANN, B. P. – YOUNG, K. A. – SCHMITZ, T. L. – BARTOW, M. J. – BAYLY, P. V., Machining Accuracy Due to Tool and Workpiece Vibrations, in *Proceedings of the 2003 ASME International Mechanical Engineering Congress and Exposition, Washington, DC*, (2003), paper no. IMECE2003-41991 (CD-ROM).
[15] MANN, B. P. – BAYLY, P. V. – DAVIES, M. A. – HALLEY, J. E., Limit Cycles, Bifurcations, and Accuracy of the Milling Process, *Journal of Sound and Vibration*, (2003), in press.
[16] PEIGNÉ, G. – PARIS, H. – BRISSAUD, D., A Model of Milled Surface Generation for Time Domain Simulation of High Speed Cutting, *Proceedings of the Institution of Mechanical Engineers Part B - Journal Of Engineering Manufacture*, **217**(7) (2003), pp. 919–930.
[17] SCHMITZ, T. L. – DAVIES, M. A. – KENNEDY, M. D., Tool Point Frequency Response Prediction for High-Speed Machining by RCSA, *Journal of Manufacturing Science and Engineering*, **123**(4) (2001), pp. 700–707.
[18] SMITH, S. – TLUSTY, J., An Overview of Modelling and Simulation of the Milling Process, *Journal of Engineering for Industry*, **113**, pp. 169–175.
[19] STÉPÁN, G., *Retarded Dynamical Systems*, Longman, Harlow, 1989.
[20] SZALAI, R. – STÉPÁN, G., Stability Boundaries of High-Speed Milling Corresponding to Period Doubling are Essentially Closed Curves, *Proceedings of ASME International Mechanical Engineering Conference and Exposition*, (2003), Washington D.C., USA, paper no. IMECE2003-42122 (CD-ROM).
[21] TIAN, J. – HUTTON, S. G., Chatter Instability in Milling Systems with Flexible Rotating Spindles – a New Theoretical Approach, *Journal of Manufacturing Science and Engineering*, **123**(1) (2001), pp. 1–9.
[22] TLUSTY, J. – POLACEK, A. – DANEK, C. – SPACEK, J., *Selbsterregte Schwingungen an Werkzeugmaschinen*, VEB Verlag Technik, Berlin, 1962.
[23] TOBIAS, S. A., *Machine Tool Vibration*, Blackie, London, 1965.
[24] WANG, J.-J. J. – ZHENG, C. M. – HUANG, C. Y., The Effect of Harmonic Force Components on Regenerative Stability in End Milling, in *Proceedings of the 2003 ASME International Mechanical Engineering Congress and Exposition, Washington, DC*, (2003), paper no. IMECE2003-42367 (CD-ROM).
[25] YOUNG, K. A. – HELVEY, A. M., Requirements for Consistent and Productive Performance in High Speed Milling, in *Proceedings of the 2003 ASME International Mechanical Engineering Congress and Exposition, Washington, DC*, (2003), paper no. IMECE2003-41694 (CD-ROM).
[26] ZHAO, M. X. – BALACHANDRAN, B., Dynamics and Stability of Milling Process, *International Journal of Solids and Structures* **38**(10–13), (2001), pp. 2233–2248.